Simple waves and shocks in a thin film of a perfectly soluble anti-surfactant solution

J Eng Math (2017) 107:167–178
DOI 10.1007/s10665-017-9924-8

Simple waves and shocks in a thin film of a perfectly soluble anti-surfactant solution

J. J. A. Conn · B. R. Duffy · D. Pritchard · S. K. Wilson · K. Sefiane

Received: 12 April 2017 / Accepted: 27 June 2017 / Published online: 3 August 2017

Abstract We consider the dynamics of a thin film of a perfectly soluble anti-surfactant solution in the limit of large capillary and Péclet numbers in which the governing system of nonlinear equations is purely hyperbolic. We construct exact solutions to a family of Riemann problems for this system, and discuss the properties of these solutions, including the formation of both simple-wave and uniform regions within the flow, and the propagation of shocks in both the thickness of the film and the gradient of the concentration of solute.

Keywords Anti-surfactant · Hyperbolic system · Marangoni effect · Riemann problems · Shocks · Simple waves

Mathematics Subject Classification 35L51 · 35L67 · 76A20 · 76D45

1 Introduction

When the molecules of a dissolved solute are preferentially expelled from the free surface of a solvent, the surface tension of the solution increases. Such solutes, which act in the opposite manner to better-known surfactants, may

J. J. A. Conn · B. R. Duffy · D. Pritchard · S. K. Wilson (✉)
Department of Mathematics and Statistics, University of Strathclyde, Livingstone Tower, 26 Richmond Street, Glasgow G1 1XH, UK
e-mail: s.k.wilson@strath.ac.uk

J. J. A. Conn
e-mail: justin.conn@strath.ac.uk

B. R. Duffy
e-mail: b.r.duffy@strath.ac.uk

D. Pritchard
e-mail: david.pritchard@strath.ac.uk

K. Sefiane
School of Engineering, University of Edinburgh, The King's Buildings, Mayfield Road, Edinburgh EH9 3FB, UK

K. Sefiane
Tianjin Key Laboratory of Refrigeration Technology, Tianjin University of Commerce, Tianjin 300134, People's Republic of China
e-mail: k.sefiane@ed.ac.uk

conveniently be referred to as "anti-surfactants". Examples of anti-surfactants include many salts, such as sodium chloride, i.e. common table salt, when added to water [1–4], water when added to short-chain alcohols [5,6], and certain resins that are included in solvent-based paints [7–10].

A fluid-dynamical model describing the behaviour of both surfactants and anti-surfactants was recently proposed by Conn et al. [11], who investigated the dependence of the surface tension σ^* of the fluid on the surface excess Γ^* of the solute. This key quantity describes the difference between the surface concentration s^* and the bulk concentration c^* [12,13]. The resulting model can describe both surfactants, molecules of which accumulate preferentially at the free surface, so that $\Gamma^* > 0$, and anti-surfactants, molecules of which preferentially accumulate in the bulk of the fluid, so that $\Gamma^* < 0$. In particular, if the surface concentration of solute is much greater than the bulk concentration, then the classical models for surfactants [14–22] are recovered.

In their original work, Conn et al. [11] considered only the linear stability of an infinitely deep layer of fluid. In contrast, in the present work, we obtain analytical solutions to the system of nonlinear equations describing the flow of a thin film of an anti-surfactant solution. In particular, we focus on the case of a "perfectly soluble" anti-surfactant, the molecules of which never adsorb to the free surface, so that the surface concentration s^* is identically zero. When both capillarity and diffusion effects are negligible, the system of equations is purely hyperbolic and admits exact solutions via the method of characteristics. Specifically, in the present work we address so-called "Riemann problems" in which the initial conditions for the film thickness and the gradient of the concentration of solute are piecewise constant (see, e.g. Whitham [23]). Note that the same system of equations arises in the flow of thin films of certain solvent-based paints [7–10], but that the problems we consider here have not previously been investigated.

In Sect. 2 we briefly describe the governing equations and their simplification in the relevant regime. In Sect. 3 we present solutions to "dry-bed" problems in which one side of the domain is initially dry, and then in Sect. 4 we present solutions to "wet-bed" problems in which there is fluid everywhere.

2 Model formulation

We consider a thin, two-dimensional film of a perfectly soluble anti-surfactant solution of constant viscosity μ^* and density ρ^* lying on top of a flat substrate. (Stars denote dimensional quantities, but dimensionless quantities will be unadorned.) We assume that the typical depth of the film H^* is much smaller than the horizontal length scale L^*, i.e. that the aspect ratio $\epsilon = H^*/L^* \ll 1$ of the film is small. Since the anti-surfactant solution is perfectly soluble, the surface concentration of solute is identically zero, and, since the film is thin, gravity effects are neglected. The dimensionless film thickness $h = h^*/H^*$ is scaled by H^*, and the bulk concentration of solute $c = c^*/C^*$ is scaled by the typical bulk concentration C^*. The velocity of the fluid is scaled to reflect the fact that flow is driven by gradients in surface tension due to gradients in the concentration of solute, i.e. by the Marangoni effect.

Adopting the natural Cartesian coordinate system and following the reduction of the model proposed by Conn et al. [11] to the thin-film regime as described by Conn [24], the governing equations for $h(x,t)$ and $c(x,t)$ are

$$\frac{\partial h}{\partial t} + \frac{\partial}{\partial x}\left(\frac{1}{3\mathrm{Ca}}h^3\frac{\partial^3 h}{\partial x^3} + \frac{1}{2}h^2\frac{\partial c}{\partial x}\right) = 0, \tag{1}$$

$$h\frac{\partial c}{\partial t} + \left(\frac{1}{3\mathrm{Ca}}h^3\frac{\partial^3 h}{\partial x^3} + \frac{1}{2}h^2\frac{\partial c}{\partial x}\right)\frac{\partial c}{\partial x} - \frac{1}{\mathrm{Pe}}\frac{\partial}{\partial x}\left(h\frac{\partial c}{\partial x}\right) = 0. \tag{2}$$

Here

$$\mathrm{Ca} = \frac{R^*T^*\eta^*C^*}{\epsilon^2\sigma^*_{\mathrm{solv}}} \quad \text{and} \quad \mathrm{Pe} = \frac{H^*R^*T^*\eta^*C^*}{\mu^*D^*} \tag{3}$$

are a capillary number and a Péclet number, respectively, in which R^* is the ideal gas constant, T^* is the (constant) temperature, η^* is the notional thickness of the free surface which is taken to be of the order of a few ångströms [11,25], σ^*_{solv} is the surface tension of the pure solvent, and D^* is the diffusivity of the solute.

When both capillarity and diffusion effects are negligible, i.e. in the limit Ca $\to \infty$ and Pe $\to \infty$, the full thin-film problem given by (1) and (2) reduces to

$$\frac{\partial h}{\partial t} + \frac{1}{2}\frac{\partial}{\partial x}\left(h^2 \frac{\partial c}{\partial x}\right) = 0, \tag{4}$$

$$\frac{\partial c}{\partial t} + \frac{1}{2} h \left(\frac{\partial c}{\partial x}\right)^2 = 0, \tag{5}$$

which express the conservation of mass of the fluid and of the solute, respectively.

Differentiating (5) with respect to x and making the substitution $\partial c/\partial x = b$, where $b(x, t)$ denotes the gradient of the concentration of solute, we obtain the equations

$$\frac{\partial h}{\partial t} + \frac{1}{2}\frac{\partial}{\partial x}(h^2 b) = 0, \tag{6}$$

$$\frac{\partial b}{\partial t} + \frac{1}{2}\frac{\partial}{\partial x}(h b^2) = 0. \tag{7}$$

Note that, because of the Marangoni effect, a positive value of b corresponds to a positive shear stress at the free surface of the film which drives the fluid to the right, and vice versa for a negative value of b.

The system of nonlinear equations given by (6) and (7) is purely hyperbolic, and so may be written in characteristic form with Riemann invariants $r_\pm = h b^{\pm 1}$, which are constant along the characteristic curves in the (x, t)-plane with slopes given by the eigenvalues $\lambda_\pm = hb(1 \pm \frac{1}{2})$. Thus

$$\frac{\mathrm{d}}{\mathrm{d}t}(r_+) = \frac{\mathrm{d}}{\mathrm{d}t}(hb) = 0, \tag{8}$$

$$\frac{\mathrm{d}}{\mathrm{d}t}(r_-) = \frac{\mathrm{d}}{\mathrm{d}t}\left(\frac{h}{b}\right) = 0 \tag{9}$$

on the characteristic curves given by

$$\frac{\mathrm{d}x}{\mathrm{d}t} = \lambda_\pm = hb\left(1 \pm \frac{1}{2}\right). \tag{10}$$

With the governing equations (4) and (5) written in the characteristic form (8)–(10), we are now able to solve a family of Riemann problems in which there is a discontinuity in the initial conditions for the film thickness h and/or the concentration gradient b. Specifically, we consider situations in which an initial discontinuity separates two otherwise uniform regions in each of which h and b are constant. Without loss of generality, we take the initial discontinuity to be at $x = 0$, and so take the initial conditions at $t = 0$ to be

$$\begin{cases} h = h_\mathrm{L}, \quad b = b_\mathrm{L} & \text{for} \quad x < 0, \\ h = h_\mathrm{R}, \quad b = b_\mathrm{R} & \text{for} \quad x > 0, \end{cases} \tag{11}$$

where, in general, none of the prescribed constants h_L, h_R, b_L and b_R are equal, and the subscripts R and L denote initial quantities to the right and to the left of the initial discontinuity, i.e. for $x > 0$ and $x < 0$, respectively. Note that since b is initially piecewise constant, c will initially be piecewise linear, and hence if $b_\mathrm{L} > 0$ and/or $b_\mathrm{R} < 0$ then c will take unphysical negative values as $x \to -\infty$ and/or $x \to \infty$. Thus in these cases the present analysis is strictly only a local (rather than a global) one. However, as we shall show, in all cases the present analysis gives valuable insight into the surprisingly complicated dynamics that can arise from an initial discontinuity.

3 The "dry-bed" problem

In this section we consider the "dry-bed" problem in which $h_{\mathrm{L}} > 0$ but $h_{\mathrm{R}} = b_{\mathrm{R}} = 0$, so that the region $x > 0$ is initially dry.

In order to construct solutions for h and b, we consider the characteristics in the (x, t)-plane given by (10). There are two characteristics emanating from any initial point $(x, 0)$, which we label as $C_{\pm}$, corresponding to the eigenvalues $\lambda_{\pm}$, respectively, and we use the superscripts R and L to denote characteristics emanating from the right and from the left of the initial discontinuity, i.e. from $x > 0$ and $x < 0$, respectively.

For $x > 0$ we have $h = b \equiv 0$ at $t = 0$, and so the $C_{\pm}^{\mathrm{R}}$ characteristics coincide and are simply vertical straight lines given by

$$C_{\pm}^{\mathrm{R}} : \; x = x_{\pm}^{\mathrm{R}}, \tag{12}$$

where $x_{\pm}^{\mathrm{R}}$ is a constant that labels each of the characteristics. On the other hand, for $x < 0$ we have $h = h_{\mathrm{L}}$ and $b = b_{\mathrm{L}}$ at $t = 0$, and so the $C_{\pm}^{\mathrm{L}}$ characteristics are inclined straight lines given by

$$C_{+}^{\mathrm{L}} : \; x = \frac{3}{2} h_{\mathrm{L}} b_{\mathrm{L}} t + x_{+}^{\mathrm{L}}, \tag{13}$$

$$C_{-}^{\mathrm{L}} : \; x = \frac{1}{2} h_{\mathrm{L}} b_{\mathrm{L}} t + x_{-}^{\mathrm{L}}, \tag{14}$$

where $x_{\pm}^{\mathrm{L}}$ are constants that label each of the characteristics. Evidently, the slopes of the $C_{\pm}^{\mathrm{L}}$ (but not the $C_{\pm}^{\mathrm{R}}$) characteristics depend on the values and signs of h_{L} and b_{L}. Physically, since h is a thickness, we are restricted to positive values of h_{L}, but, since b is a concentration gradient, b_{L} can be either positive or negative, and we now consider these possibilities in turn.

3.1 The dry-bed problem with $b_{\mathrm{L}} < 0$

Firstly, consider the case $b_{\mathrm{L}} < 0$ in which a negative concentration gradient drives the fluid to the left. In this case, the $C_{\pm}^{\mathrm{L}}$ characteristics have a negative slope, and hence the information carried by these characteristics propagates to the left.

Figure 1 shows the typical arrangement of the characteristics in the (x, t)-plane in this case. Three separate regions are identified, namely a uniform region to the left (labelled $\mathrm{U_L}$), a uniform region to the right (labelled $\mathrm{U_R}$), and a simple-wave region (labelled SW). The dashed lines correspond to the $C_{\pm}^{\mathrm{R}}$ characteristics in region $\mathrm{U_R}$ and the C_{-}^{L} characteristics in region $\mathrm{U_L}$, the thin solid lines correspond to the C_{+}^{L} characteristics in region $\mathrm{U_L}$ and the C_{+} characteristics which form the expansion fan in region SW, and the thick solid lines represent the limiting characteristics which form the boundaries of region SW. We now construct the solutions that hold in each of these regions.

Region $\mathrm{U_L}$ corresponds to the uniform region of undisturbed fluid to the left, i.e. extending to $x \to -\infty$, with the right-hand boundary of region $\mathrm{U_L}$ being the limiting C_{+}^{L} characteristic, i.e. the straight line given by (13) with $x_{+}^{\mathrm{L}} = 0$. The solutions for h and b in region $\mathrm{U_L}$ are therefore simply

$$h = h_{\mathrm{L}}, \quad b = b_{\mathrm{L}} \, (<0) \quad \text{for} \quad x \le \frac{3}{2} h_{\mathrm{L}} b_{\mathrm{L}} t \, (< 0). \tag{15}$$

The corresponding solution for c is obtained by integrating $\partial c / \partial x = b_{\mathrm{L}}$ with respect to x and (5) with respect to t to obtain

$$c = c_{\mathrm{L}} + b_{\mathrm{L}} x - \frac{1}{2} h_{\mathrm{L}} {b_{\mathrm{L}}}^2 t \quad \text{for} \quad x \le \frac{3}{2} h_{\mathrm{L}} b_{\mathrm{L}} t \, (< 0), \tag{16}$$

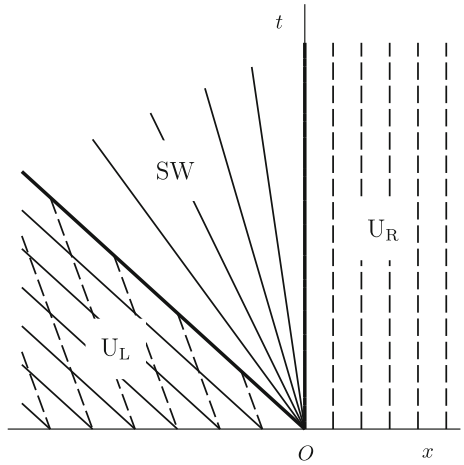

Fig. 1 The typical arrangement of the characteristics in the (x, t)-plane for the dry-bed problem with $b_{\mathrm{L}} < 0$. Three separate regions are identified, namely a uniform region to the left (labelled $\mathrm{U_L}$), a uniform region to the right (labelled $\mathrm{U_R}$), and a simple-wave region (labelled SW). The *dashed lines* correspond to the $C_{\pm}^{\mathrm{R}}$ characteristics in region $\mathrm{U_R}$ and the C_{-}^{L} characteristics in region $\mathrm{U_L}$, the *thin solid lines* correspond to the C_{+}^{L} characteristics in region $\mathrm{U_L}$ and the C_+ characteristics which form the expansion fan in region SW, and the *thick solid lines* represent the limiting characteristics which form the boundaries of region SW

where c_{L} is a constant of integration.

Similarly, region $\mathrm{U_R}$ corresponds to the uniform region with no fluid to the right of $x = 0$, i.e. extending from $x = 0$ to $x \to \infty$. The solutions for h, b and c in region $\mathrm{U_R}$ are therefore simply

$$h \equiv 0, \quad b \equiv 0, \quad c \equiv 0 \quad \text{for} \quad x \geq 0. \tag{17}$$

The C_{-}^{L} characteristics emanating from region $\mathrm{U_L}$ intersect the limiting C_{+}^{L} characteristic, and then enter region SW. Since these characteristics carry the same value of $r_- = r_-^{\mathrm{L}}$ in both regions, we have

$$\frac{h}{b} = \frac{h_{\mathrm{L}}}{b_{\mathrm{L}}} \quad \text{in region SW.} \tag{18}$$

Furthermore, since each C_+ characteristic carries a constant value of r_+, we also have

$$hb = k \quad \text{in region SW} \tag{19}$$

for some constant k that is different on each C_+ characteristic in region SW. Solving Eqs. (18) and (19) shows that both h and b are constant along any given C_+ characteristic in region SW. Thus λ_+ must be constant for any value of k and, from (10), the C_+ characteristics in region SW must be straight lines through the origin of the (x, t)-plane with slopes depending on the value of k. These C_+ characteristics form the expansion fan in region SW shown in Fig. 1. Furthermore, since all C_+ characteristics are straight lines, we may write

$$\frac{\mathrm{d}x}{\mathrm{d}t} = \frac{x}{t} = \frac{3}{2}hb. \tag{20}$$

Solving Eqs. (18) and (20), we find the simple-wave solutions for h and b in region SW to be

$$h = \sqrt{\frac{2h_{\mathrm{L}}x}{3b_{\mathrm{L}}t}}, \quad b = -\sqrt{\frac{2b_{\mathrm{L}}x}{3h_{\mathrm{L}}t}} \; (< 0), \tag{21}$$

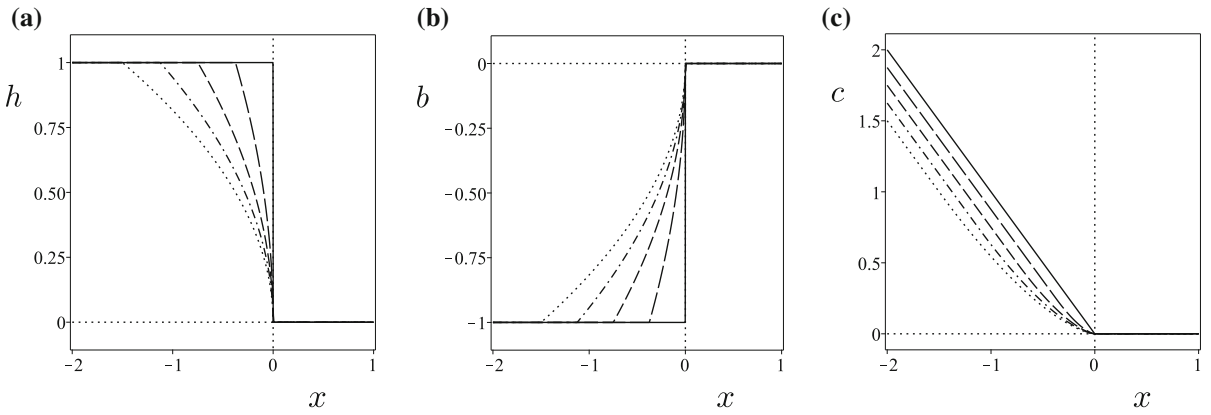

Fig. 2 Exact solutions of the dry-bed problem with $b_{\mathrm{L}} < 0$ given by Eqs. (15)–(17), (21) and (22) for **a** h, **b** b and **c** c with initial conditions (11), where $h_{\mathrm{R}} = 0$, $b_{\mathrm{R}} = 0$, $h_{\mathrm{L}} = 1$, $b_{\mathrm{L}} = -1$ and $c_{\mathrm{L}} = 0$, for $t = 0, 0.25, 0.5, 0.75, 1$ (*solid* to *dotted lines*, respectively)

where we have chosen the signs of the square roots appearing in h and b appropriately.

The corresponding simple-wave solution for c in region SW which is continuous with the solution in region $\mathrm{U_L}$ across the limiting C_+^{L} characteristic, i.e. across $x = 3h_{\mathrm{L}}b_{\mathrm{L}}t/2$, is

$$c = c_{\mathrm{L}} + \left(\frac{2}{3}\right)^{3/2} \sqrt{\frac{b_{\mathrm{L}}x^3}{h_{\mathrm{L}}t}}. \tag{22}$$

The presence of the arbitrary constant, namely c_{L}, in the solution for c reflects the fact that adding a uniform amount of solute to the film has no effect on the dynamics of the system, i.e. only gradients in the concentration of solute affect the behaviour of the film.

Figure 2 shows typical plots of the exact solutions given by (15)–(17), (21) and (22), and, in particular, shows the uniform solutions to the right and to the left and the simple-wave solutions that connect them. Since b is always negative, the negative concentration gradient always drives the fluid to the left, advecting the solute with it. Note that, since gravity, capillarity and diffusion effects have all been neglected, there is no physical mechanism to drive the fluid rightwards, and so the initially dry region $x > 0$ always remains dry.

3.2 The dry-bed problem with $b_{\mathrm{L}} > 0$

Secondly, consider the case $b_{\mathrm{L}} > 0$ in which a positive concentration gradient drives the fluid to the right. In this case, the $C_{\pm}^{\mathrm{R}}$ characteristics, given by (12), are again vertical straight lines, but the $C_{\pm}^{\mathrm{L}}$ characteristics, given by (13) and (14), now have a positive slope. The C_+ and C_- characteristics therefore intersect at the origin of the (x, t)-plane, meaning that shocks form instantly (i.e. at $t = 0$) in both h and b at $x = 0$, and for $t > 0$ these shocks propagate with some speed $\dot{x}_{\mathrm{s}}$. The speed of the shocks $\dot{x}_{\mathrm{s}}$ is determined using the Rankine–Hugoniot shock conditions [23] for this problem, namely

$$\dot{x}_{\mathrm{s}} [\![h]\!] = \frac{1}{2} \left[\!\left[h^2 b\right]\!\right], \tag{23}$$

$$\dot{x}_{\mathrm{s}} [\![b]\!] = \frac{1}{2} \left[\!\left[hb^2\right]\!\right], \tag{24}$$

where the notation $[\![u]\!]$ denotes the jump in the quantity u across the shock. Solving (23) and/or (24) yields

$$\dot{x}_{\mathrm{s}} = \frac{1}{2} h_{\mathrm{L}} b_{\mathrm{L}} \ (> 0), \tag{25}$$

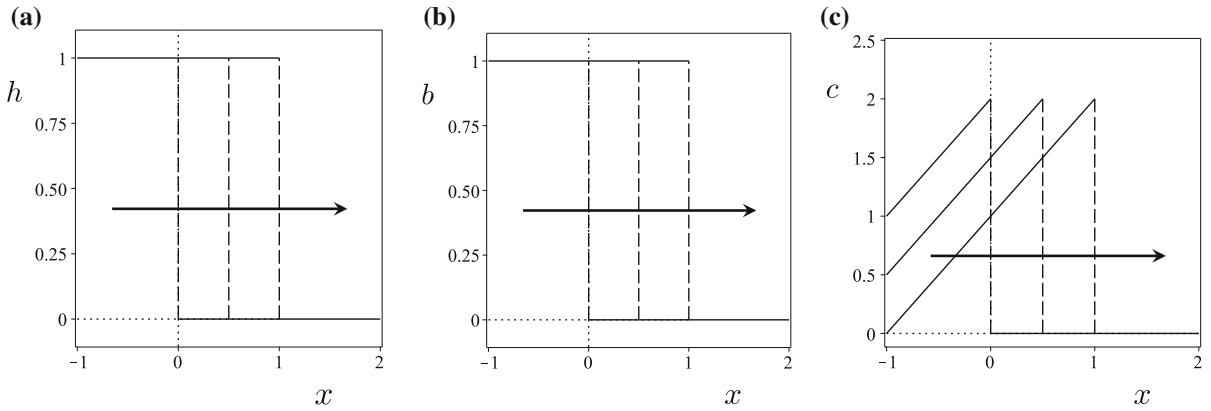

Fig. 3 Exact solutions of the dry-bed problem with $b_{\mathrm{L}} > 0$ given by Eq. (26) for **a** h, **b** b and **c** c with initial conditions (11), where $h_{\mathrm{R}} = 0$, $b_{\mathrm{R}} = 0$, $h_{\mathrm{L}} = 1$, $b_{\mathrm{L}} = 1$ and $c_{\mathrm{L}} = 2$, for $t = 0, 1, 2$. The *arrows* indicate the rightwards propagation of the shocks, which are indicated with *dashed lines*

showing that the location of the shocks is given by the limiting C_{-}^{L} characteristic. It is then straightforward to obtain the solutions for h, b and c, namely

$$\begin{cases} h = h_{\mathrm{L}}, \quad b = b_{\mathrm{L}}\ (>0), \quad c = c_{\mathrm{L}} + b_{\mathrm{L}}x - \frac{1}{2}h_{\mathrm{L}}{b_{\mathrm{L}}}^2 t & \text{for} \quad x < \frac{1}{2}h_{\mathrm{L}}b_{\mathrm{L}}t\ (>0), \\ h \equiv 0, \quad b \equiv 0, \quad c \equiv 0 & \text{for} \quad x > \frac{1}{2}h_{\mathrm{L}}b_{\mathrm{L}}t\ (>0), \end{cases} \tag{26}$$

which simply represent uniform solutions for h and b and a linear solution for c, terminated by shocks that propagate rightwards at constant speed $\dot{x}_{\mathrm{s}}$ given by (25).

Figure 3 shows typical plots of the exact solutions given by (26), and, in particular, shows the rightwards propagation of the shocks. Note that, in contrast to the case $b_{\mathrm{L}} < 0$ shown on Fig. 2, in this case the positive concentration gradient provides a physical mechanism that can drive the fluid rightwards into the initially dry region $x > 0$.

4 The "wet-bed" problem

In this section we consider the "wet-bed" problem in which $h_{\mathrm{L}} > 0$ and $h_{\mathrm{R}} > 0$, so that there is initially fluid everywhere. Since there are now four (rather than two) free parameters, there are more cases to consider than for the dry-bed problem. However, for brevity, in the present work we consider only two of the more interesting cases, in both of which $h_{\mathrm{L}} > h_{\mathrm{R}} > 0$, $b_{\mathrm{L}} < 0$ and $b_{\mathrm{R}} < 0$. In particular, in Sect. 4.1 we consider the case $h_{\mathrm{L}}b_{\mathrm{L}} < h_{\mathrm{R}}b_{\mathrm{R}}$ and show that the solution to this problem resembles that of the classical Stoker problem [26] in which a simple-wave solution continuously connects two uniform regions, the rightmost of which is connected by a shock to a further uniform region, while in Sect. 4.2 we consider the case $h_{\mathrm{L}}b_{\mathrm{L}} > h_{\mathrm{R}}b_{\mathrm{R}}$ and show that the solution to this problem consists of three uniform regions connected by two shocks. In both cases, as in the case of the dry-bed problem discussed in Sect. 3.1, since b is always negative, the negative concentration gradient always drives the fluid to the left, and so the solution in the region $x > 0$ always remains at its initial values.

4.1 Wet-bed problem with $h_{\mathrm{L}}b_{\mathrm{L}} < h_{\mathrm{R}}b_{\mathrm{R}}$

Firstly, we consider the case $h_{\mathrm{L}}b_{\mathrm{L}} < h_{\mathrm{R}}b_{\mathrm{R}}$. For $x > 0$, we have $h = h_{\mathrm{R}}$ and $b = b_{\mathrm{R}}$ at $t = 0$, and so the $C_{\pm}^{\mathrm{R}}$ characteristics are straight lines given by

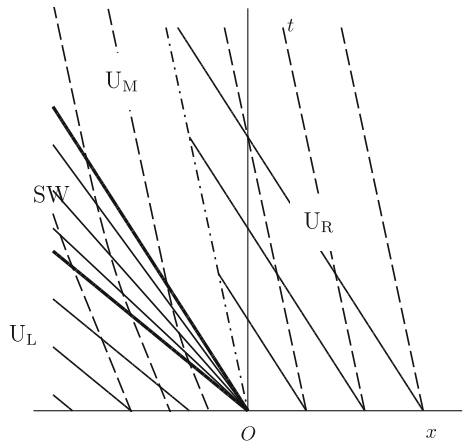

Fig. 4 The typical arrangement of the characteristics in the (x, t)-plane for the wet-bed problem with $h_L > h_R > 0$, $b_L < 0$, $b_R < 0$ and $h_L b_L < h_R b_R$. In addition to two uniform regions and one simple-wave region similar to those that occur in the dry-bed problem (again labelled U_L, U_R and SW, respectively), we also identify an additional "middle" uniform region (labelled U_M), not present in the dry-bed problem, that connects the simple-wave solutions in region SW to the uniform solutions in region U_R via a shock (indicated with the *dash-dot line*)

$$C_+^R : x = \frac{3}{2} h_R b_R t + x_+^R, \tag{27}$$

$$C_-^R : x = \frac{1}{2} h_R b_R t + x_-^R, \tag{28}$$

where $x_\pm^R$ are constants that label each of the characteristics. For $x < 0$ we have $h = h_L$ and $b = b_L$ at $t = 0$, and so the $C_\pm^L$ characteristics are, as in the dry-bed problem, straight lines given by (13) and (14). From the forms of these characteristics, it is clear that if the constraint $h_L b_L < h_R b_R$ did *not* hold, then the slope of the C_+^R characteristics would be shallower than that of the C_+^L characteristics, and the C_+ characteristics would therefore intersect at the origin of the (x, t)-plane, meaning that shocks would form instantly in both h and b at $x = 0$. This is the situation considered in Sect. 4.2.

Figure 4 shows the typical arrangement of the characteristics in the (x, t)-plane for the wet-bed problem in the case $h_L b_L < h_R b_R$. In addition to two uniform regions and one simple-wave region similar to those that occur in the dry-bed problem (again labelled U_L, U_R and SW, respectively), we also identify an additional "middle" uniform region (labelled U_M), not present in the dry-bed problem, that connects the simple-wave solutions in region SW to the uniform solutions in region U_R via a shock (indicated with the dash-dot line). We now construct the solutions that hold in each of these regions.

The solutions for h, b and c in the uniform regions U_L and U_R are simply

$$h = h_L, \quad b = b_L\,(< 0), \quad c = c_L + b_L x - \frac{1}{2} h_L {b_L}^2 t \quad \text{for} \quad x \le \frac{3}{2} h_L b_L t\,(< 0) \tag{29}$$

and

$$h = h_R, \quad b = b_R\,(< 0), \quad c = c_R + b_R x - \frac{1}{2} h_R {b_R}^2 t \quad \text{for} \quad x \ge \frac{3}{2} h_R b_R t\,(< 0), \tag{30}$$

respectively, where c_L and c_R are constants of integration.

As in the case of the dry-bed problem, the C_-^L characteristics emanating from region U_L enter region SW, and so the solutions for h and b in this region are precisely the same as those in the dry-bed problem given by (21) and (22), respectively. However, in contrast to the dry-bed problem, the right-hand boundary of region SW is not simply the vertical line $x = 0$, but now must be found as part of the solution. Using the solutions for h and b in region SW, the C_-^L characteristics in this region satisfy

$$\frac{\mathrm{d}x}{\mathrm{d}t} = \frac{x}{3t}, \tag{31}$$

and hence are given by

$$t = \beta x^3, \tag{32}$$

where the constant of integration β (< 0) must be negative in order that the C_-^{L} characteristics be continuous across the boundary between regions $\mathrm{U_L}$ and SW. After passing through region SW, the C_-^{L} characteristics eventually intersect the boundary between regions SW and $\mathrm{U_M}$, and then enter region $\mathrm{U_M}$. Since these characteristics carry the same value of $r_- = r_-^{\mathrm{L}}$ in both regions, we have

$$\frac{b}{h} = \frac{b_{\mathrm{L}}}{h_{\mathrm{L}}} \quad \text{in region } \mathrm{U_M}. \tag{33}$$

However, there are no solutions for the uniform values of h and b in region $\mathrm{U_M}$, denoted by h_{M} and b_{M}, that are continuous with the solutions in region $\mathrm{U_R}$ given by (30), and so there must be shocks in h and b at the boundary between regions $\mathrm{U_M}$ and $\mathrm{U_R}$. The uniform values of h and b on either side of the shocks are related by the shock conditions (23) and (24), which, along with (33), give three simultaneous (nonlinear) algebraic equations for three unknowns, namely the shock speed $\dot{x}_{\mathrm{s}}$, h_{M} and b_{M}. Solving these equations yields

$$\dot{x}_{\mathrm{s}} = \frac{1}{2} h_{\mathrm{R}} b_{\mathrm{R}} \ (< 0), \tag{34}$$

showing that the location of the shocks is given by the limiting C_-^{R} characteristic, and the uniform solutions for h and b in region $\mathrm{U_M}$, namely

$$h_{\mathrm{M}} = \sqrt{\frac{h_{\mathrm{L}} h_{\mathrm{R}} b_{\mathrm{R}}}{b_{\mathrm{L}}}}, \quad b_{\mathrm{M}} = -\sqrt{\frac{h_{\mathrm{R}} b_{\mathrm{L}} b_{\mathrm{R}}}{h_{\mathrm{L}}}} \ (< 0). \tag{35}$$

The solution for c in region $\mathrm{U_M}$, denoted by c_{M}, which is continuous with the solution in region SW, is

$$c_{\mathrm{M}} = c_{\mathrm{L}} + \sqrt{\frac{h_{\mathrm{R}} b_{\mathrm{L}} b_{\mathrm{R}}}{h_{\mathrm{L}}}} \left(\frac{h_{\mathrm{R}} b_{\mathrm{R}} t}{2} - x \right). \tag{36}$$

Requiring that the solution for c (but not, of course, the solutions for h and b) is also continuous across the boundary between regions $\mathrm{U_M}$ and $\mathrm{U_R}$, i.e. across $x = \frac{1}{2} h_{\mathrm{R}} b_{\mathrm{R}} t$, shows that $c_{\mathrm{R}} = c_{\mathrm{L}}$, i.e. that, as in the dry-bed case, there is a single arbitrary constant, namely c_{L}, in the solution for c which has no effect on the dynamics of the system.

Figure 5 shows typical plots of the exact solutions for h, b and c given by (21), (22), (29), (30), (35) and (36). In particular, Fig. 5 shows that the solutions for both h and b are continuous everywhere except for shocks at the boundary between region $\mathrm{U_M}$ and region $\mathrm{U_R}$, which propagate leftwards into the region $x < 0$ at constant speed $\dot{x}_{\mathrm{s}}$ given by (34).

4.2 Wet-bed problem with $h_{\mathrm{L}} b_{\mathrm{L}} > h_{\mathrm{R}} b_{\mathrm{R}}$

Secondly, we consider the case $h_{\mathrm{L}} b_{\mathrm{L}} > h_{\mathrm{R}} b_{\mathrm{R}}$, i.e. the case in which the C_+ characteristics intersect at the origin of the (x, t)-plane, meaning that shocks form instantly in both h and b at $x = 0$. In fact, it is immediately apparent that in this case there must be *two* shocks (rather than just one shock) in both h and b. Specifically, since the values h_{L},

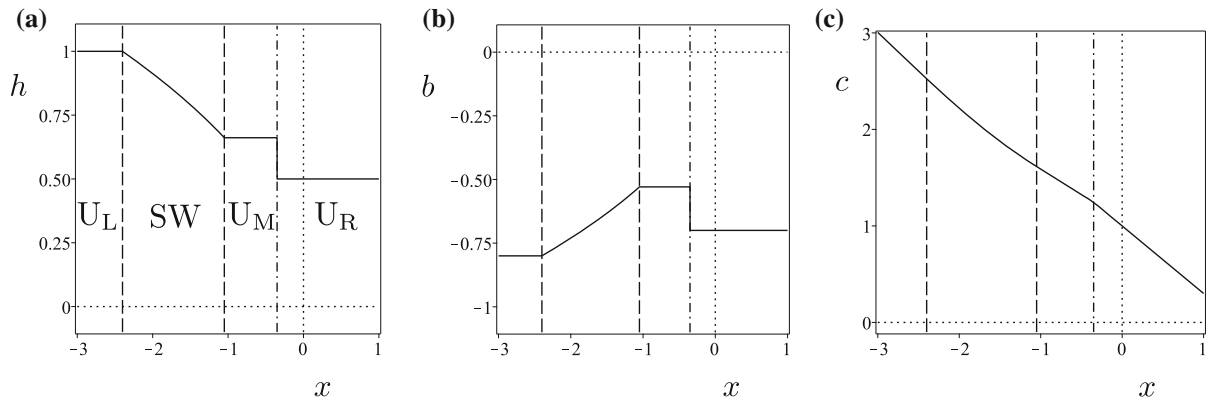

Fig. 5 Exact solutions of the wet-bed problem with $h_L > h_R > 0$, $b_L < 0$, $b_R < 0$ and $h_L b_L < h_R b_R$ given by (21), (22), (29), (30), (35) and (36) for **a** h, **b** b and **c** c, where $h_L = 1$, $b_L = -0.8$, $h_R = 0.5$, $b_R = -0.7$ and $c_L = 1$, at $t = 2$. The boundaries between the regions are indicated with *dashed lines*, except for the locations of the shocks at the boundary between regions U_M and U_R, which are indicated with *dash-dot lines*

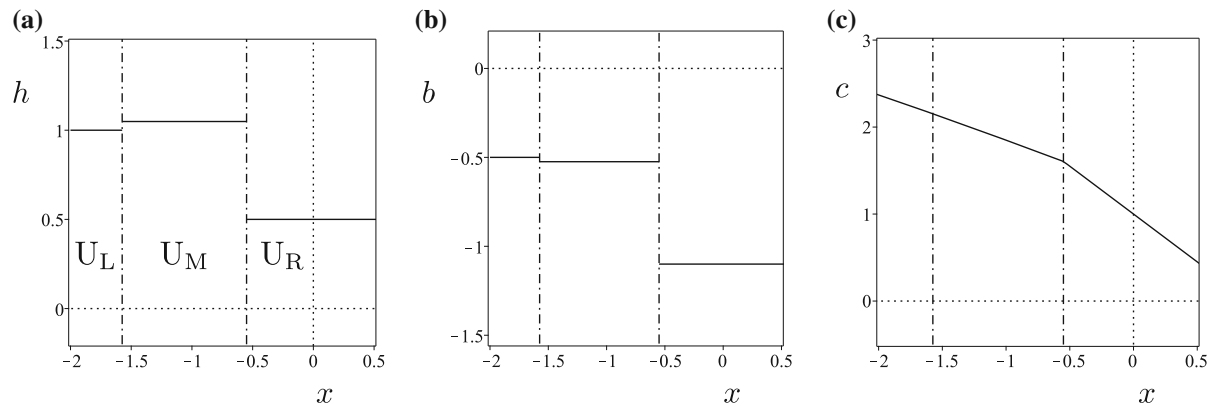

Fig. 6 Exact solutions of the wet-bed problem with $h_L > h_R > 0$, $b_L < 0$, $b_R < 0$ and $h_L b_L > h_R b_R$ given by (29), (30), (35) and (36) for **a** h, **b** b and **c** c, where $h_L = 1$, $b_L = -0.5$, $h_R = 0.5$, $b_R = -1.1$ and $c_L = 1$, at $t = 1$. The shocks at the boundaries between regions U_L and U_M and between regions U_M and U_R are indicated with *dash-dot lines*

b_L, h_R and b_R are all prescribed, a single shock in both h and b would introduce only a single unknown (namely, the single shock speed), leading to an over-determined system, and so a second shock with a second shock speed must also occur in both h and b.

Proceeding along the same lines as in the cases discussed previously, we find that the solution in this case consists of the uniform regions U_L and U_R in which the solutions for h, b and c are again given by (29) and (30) separated by a middle uniform region U_M in which the solutions for h, b and c are again given by (35) and (36). Solving the appropriate shock conditions yields

$$\dot{x}_s^{LM} = \frac{1}{2}\left(h_L b_L + h_R b_R - \sqrt{h_L h_R b_L b_R}\right) \ (< 0) \tag{37}$$

and

$$\dot{x}_s^{MR} = \frac{1}{2} h_R b_R \ (< 0), \tag{38}$$

where $\dot{x}_s^{LM}$ and $\dot{x}_s^{MR}$ denote the speeds of the shocks at the boundaries of regions U_L and U_M and regions U_M and U_R, respectively. Note that $|\dot{x}_s^{LM}| > |\dot{x}_s^{MR}|$, and so the middle region gets monotonically wider as t increases, and, in particular, the shocks never collide. Furthermore, comparing the solutions in the three different regions reveals that whereas the value of b_M always lies between b_L and b_R, the value of h_M is always greater than *both* h_L and h_R, i.e. the film is always thickest in the middle region.

Figure 6 shows typical plots of the exact solutions for h, b and c given by (29), (30), (35) and (36). In particular, Fig. 6 shows that the solutions for both h and b are uniform everywhere except at the shocks, which propagate leftwards into the region $x < 0$ at constant speeds $\dot{x}_s^{LM}$ and $\dot{x}_s^{MR}$ given by (37) and (38), respectively. Figure 6 also shows that the film is thickest in the middle region between the two shocks.

5 Conclusions

We constructed exact solutions to a family of Riemann problems that describe the dynamics of a thin film of a perfectly soluble anti-surfactant solution in the limit of large capillary and Péclet numbers. These solutions describe the formation of both simple-wave and uniform regions within the flow, and the propagation of shocks in both the thickness of the film and the gradient of concentration of solute.

While the solutions obtained in the present work are for a somewhat idealised situation, and, as discussed at the end of Sect. 2, in some cases are strictly only local solutions valid sufficiently close to the location of the initial discontinuity, they nevertheless provide an interesting analytical insight into the surprisingly complicated dynamics that can occur in this relatively simple system, and hint at even richer dynamics in the full thin-film problem given by (1) and (2). Specifically, the present solutions provide an excellent illustration of fundamental differences between surfactant and anti-surfactant dynamics: the differences between the advective transport terms for bulk and for surface concentration of solute mean that equivalent solutions are not available for thin films laden with surfactants. More pragmatically, the present solutions also provide a valuable analytical benchmark against which numerical solutions of the full thin-film problem can be validated in the future.

Acknowledgements During the course of the present work, JJAC was supported by a University of Strathclyde Postgraduate Research Scholarship, and SKW was partially supported by Leverhulme Trust Research Fellowship RF-2013-355.

References

1. Long FA, Nutting GC (1942) The relative surface tension of potassium chloride solutions by a differential bubble pressure method. J Am Chem Soc 64:234–243
2. Shaw DJ (1970) Introduction to colloid and surface chemistry. Butterworths, Oxford
3. Li Z, Lu BC-Y (2001) Surface tension of aqueous electrolyte solutions at high concentrations–representation and prediction. Chem Eng Sci 56:2879–2888
4. Ozdemir O, Karakashev SI, Nguyen AV, Miller JD (2009) Adsorption and surface tension analysis of concentrated alkali halide brine solutions. Miner Eng 22:263–271
5. Vázquez G, Alvarez E, Navaza JM (1995) Surface tension of alcohol + water from 20 to 50 degrees C. J Chem Eng Data 40:611–614
6. Hernández-Sánchez JF, Eddi A, Snoeijer JH (2015) Marangoni spreading due to a localized alcohol supply on a thin water film. Phys Fluids 27:032003
7. Overdiep WS (1986) The levelling of paints. Prog Org Coat 14:159–175
8. Wilson SK (1993) The levelling of paint films. IMA J Appl Math 50:149–166
9. Howison SD, Moriarty JA, Ockendon JR, Terrill EL, Wilson SK (1997) A mathematical model for drying paint layers. J Eng Math 32:377–394
10. Eres MH, Weidner DE, Schwartz LW (1999) Three-dimensional direct numerical simulation of surface-tension-gradient effects on the leveling of an evaporating multicomponent fluid. Langmuir 15:1859–1871

11. Conn JJA, Duffy BR, Pritchard D, Wilson SK, Halling PJ, Sefiane K (2016) Fluid-dynamical model for antisurfactants. Phys Rev E 93:043121
12. Mitropoulos AC (2008) What is a surface excess? J Eng Sci Technol Rev 1:1–3
13. Langevin D (2014) Rheology of adsorbed surfactant monolayers at fluid surfaces. Annu Rev Fluid Mech 46:47–65
14. Borgas MS, Grotberg JB (1988) Monolayer flow on a thin film. J Fluid Mech 193:151–170
15. Jensen OE, Grotberg JB (1992) Insoluble surfactant spreading on a thin viscous film: shock evolution and film rupture. J Fluid Mech 240:259–288
16. Jensen OE, Grotberg JB (1993) The spreading of heat or soluble surfactant along a thin liquid film. Phys Fluids A 5:58–68
17. Matar OK, Troian SM (1999) The development of transient fingering patterns during the spreading of surfactant coated films. Phys Fluids 11:3232–3246
18. Edmonstone BD, Matar OK, Craster RV (2004) Flow of surfactant-laden thin films down an inclined plane. J Eng Math 50:141–156
19. Warner MRE, Craster RV, Matar OK (2004) Fingering phenomena created by a soluble surfactant deposition on a thin liquid film. Phys Fluids 16:2933–2951
20. Levy R, Shearer M (2006) The motion of a thin liquid film driven by surfactant and gravity. SIAM J Appl Math 66:1588–1609
21. Levy R, Shearer M, Witelski TP (2007) Gravity-driven thin liquid films with insoluble surfactant: smooth traveling waves. Eur J Appl Math 18:679–708
22. Escher J, Hillairet M, Laurencot P, Walker C (2012) Weak solutions to a thin film model with capillary effects and insoluble surfactant. Nonlinearity 25:2423–2441
23. Whitham GB (1974) Linear and Nonlinear Waves. Wiley, New York
24. Conn JJA (2017) Stability and dynamics of anti-surfactant solutions. Ph.D. thesis, Department of Mathematics and Statistics, University of Strathclyde, Glasgow
25. Chang C-H, Franses EI (1995) Adsorption dynamics of surfactants at the air/water interface: a critical review of mathematical models, data, and mechanisms. Colloids Surf A 100:1–45
26. Stoker JJ (1957) Water Waves. Interscience Publishers Inc, New York